



## Kinetics, thermodynamics and equilibrium evaluation of adsorptive removal of iron from aqueous solution onto Algerian biosorbent 'LUFFA CYLINDRICA'

C. Ad<sup>1,\*</sup>, M. Benalia<sup>1</sup>, Y. Laidani<sup>2</sup>, H. Elmsellem<sup>3,\*</sup>, G. Henini<sup>2</sup>, I. Nouacer<sup>1</sup>, M. Djedid<sup>1</sup>

<sup>1</sup>Laboratory of process engineering, Department Process Engineering, Laghouat University, P.O Box 37G, Route de Ghardaïa, 03000, Laghouat, Algeria.

<sup>2</sup>Laboratory Environment-Water, Department Process Engineering, Chlef University, P.O Box. 151, Hay Essalem 02000 Chlef, Algeria.

<sup>3</sup>LCAE-URAC18, Laboratory of Applied Chemistry and Environment, Department of Chemistry, Faculty of Sciences, Mohamed 1st University, Oujda, Morocco.

Received 21 Nov 2015, Revised 05 Jan 2016, Accepted 12 Jan 2016

\*Corresponding : E-mail: [chiffaad@gmail.com](mailto:chiffaad@gmail.com) / [h.elmsellem@yahoo.fr](mailto:h.elmsellem@yahoo.fr); Tel: (+213662080340) / (+212670923431)

### Abstract

This study was focused on the adsorption of iron (II) on the cords of Luffa Cylindrica fibers, LC, as an Algerian biosorbent in the batch equilibrium. The vibrational characteristics, morphological, and structural of the LC are effectuated by Fourier transform infra red spectroscopy (FT-IR) studies and by x-ray diffraction (XRD) before and after adsorption. Kinetic models, thermodynamic studies, and four types of adsorption isotherms: Langmuir, Freundlich, Temkin and Dubinin–Radushkevich, were used to describe this phenomenon of adsorption. It was studied the influence of various parameters such as: the time of contact, pH, initial concentration, effect of masse and particles size of the biosorbent. Experimental results were shown that iron adsorption depends mainly on the pH and the initial concentration of the iron (II) in solution. Langmuir model is most representative for the adsorption of iron(II) on LC cords. The pseudo-second-order rate equation described the Kinetic data well. The examination of the thermodynamic analysis shows that the reaction is exothermic ( $\Delta H^\circ < 0$ ), negative value of entropy ( $\Delta S^\circ$ ) indicates that there is a decrease in the messy interface solution system (solid / solute) during the adsorption process. Negative values of Gibbs energy ( $\Delta G^\circ$ ) show that the adsorption process is spontaneous.

**Keywords:** Luffa Cylindrica, adsorption, iron, characterization, kinetics, Isotherms.

### 1. Introduction

One of the main environmental issues today is related to water contamination by effluents and potentially toxic metals and their cumulative effects on biota [1]. According to the toxicity of these metals and their dangerous effects on the environment and human health, many attempts have been done to remove them from waste water and environment.

Most of heavy metals above trace quantities are harmful to humans, animals and plants [2]. Iron is one of the major constituents of the lithosphere and comprises approximately 5% of it. It is routinely detected in municipal waste effluent, particularly in cities where iron and steel are manufactured. Iron readily complexes with sulphates in the sediments of many surface levels of water. The primary concern about the presence of iron in drinking water is its objectionable taste. The taste of iron in drinking water can be easily detected even at low concentrations of about 1.8 mg/L [3].

There are many problems that result from iron toxicity. These include anorexia, oliguria, diarrhoea, hypothermia, diphasic shock, metabolic acidosis and even death. In addition to these, the patient may experience vascular congestion of the gastrointestinal tract, liver, kidneys, heart, brain, adrenals and thymus.

With acute iron poisoning, much of the damage happens to the gastrointestinal tract and liver which may result from the high localized iron concentration and free radical production leading to hepatic toxicity via lipid peroxidation and destruction of the hepatic mitochondria. As a result of iron storage disease, the liver becomes cirrhotic. Hepatoma, a primary cancer of the liver, has become the most common cause for death among patients with hemochromatosis [4].

This is an iron storage disease that results from the inability of the intestine to keep out unwanted iron. Instead, this iron accumulates in the liver causing siderosis and causes damage to the storage organs. Also, when siderosis becomes severe in young people, it leads to myocardial disease which is a common cause of death. Impotence may also occur in young men and amenorrhea in young women. Both these problems relating to reproduction are due to iron loading in the anterior pituitary [5].

Among the most appropriate current processes for treating effluent charged heavy metal ions are membrane techniques such as; osmosis, electrodialysis, ultrafiltration, microfiltration and nanofiltration. Although these techniques are methods of choice for removing heavy metal ions they have the disadvantage of being little selective and high consumers of energy. Adsorption is one of the simple, effective, economic methods and most useful for the removal of the pollutants of waste water [6].

*Luffa cylindrica*, LC, mainly consists of cellulose, hemicelluloses and lignin; of composition (60%, 30% and 10% by weight, respectively) [7]. Cellulose structure consists of monomeric unit of a  $\beta$ -D-glucopyranose linked through 1,4-glucosidic linkage. Cellulose is a renewable, cheap, low in density, biodegradable material and exhibits better processing flexibility. Cellulose is a highly functionalized, linear stiff chain homopolymer, characterized by its hydrophilicity, chirality, biodegradability and broad chemical modifying capacity [8]. Because of its unique structure, LC has been used as an efficient adsorbent or as a carrier for immobilization of some microalgal cells for the removal of water pollutants [9, 10]. In this study, LC fibers were investigated as an alternative biosorbent for removing of iron from aqueous solutions.

The adsorption of Fe (II) ions by the LC was investigated under different experimental conditions, including the contact time, pH, and concentration of iron in solution and dose of LC. For studying the efficiency of LC in removing Fe (II) from aqueous solution; kinetic and thermodynamic parameters and four types of adsorption isotherms: Langmuir, Freundlich, Temkin and Dubinin–Radushkevich were represented to describe well the adsorption. Physical and chemical characteristics of LC were characterized before and after adsorption using FT-IR and XRD.

1

## **2. Materials and methods :**

### *2.1. Adsorbent preparation:*

*Luffa cylindrica* (LC) was purchased from a local specialty shop in Algeria. A quantity of cords LC was taken, washed and boiled in distilled water for 30 min, after that was filtered and rinsed in distilled water; finally the cords were dried at 105°C for 120 min [11]. If the optical density of juice is higher than the optical density of water; the cords should boil again till the optical density of juice is equal to the optical density of water.

### *2.2. Preparation of metal solutions:*

All the chemicals used were of analytical reagent (AR) grade. Stock solution of 1000 mg/L of Fe (II) was prepared from 5.028 g of  $\text{FeSO}_4 \cdot 7\text{H}_2\text{O}$  in 1000  $\text{cm}^3$  distilled water. Desired test solutions of Fe (II) ions were prepared using appropriate subsequent dilutions of the stock solution. The range of concentrations of Fe (II) ions were prepared from standard solution varied between 10 and 100mg/L. The pH of the solution was adjusted with  $\text{H}_2\text{SO}_4$  or NaOH solution 0.1 M by using a pH meter.

### *2.3. Analysis:*

Fourier Transform Infrared Spectroscopy, FTIR (IRPrestige-21, Shimadzu, Japan) was used to identify the different chemical functional groups present in the LC. The analysis was carried out using KBr and the spectral range varying from 4000 to 600 $\text{cm}^{-1}$ . The FTIR spectra of the free unloaded LC were compared with those obtained for LC loaded with iron. Powder diffractograms of the LC samples were obtained with an X'Pert PHILIPS diffractometer with PW3373/00Cu LFF radiation at 40 kV and 50 mA. The diffractograms were used to identify the compounds and to verify crystalline structure. They were compared with LC loaded with Fe (II). Diffractograms were obtained by varying angle ( $2\theta$ ) from 5° to 60°.

#### 2.4. Adsorption Experiments:

The adsorption experiments were carried out by batch process. 1 g of biosorbent was placed in erlenmeyer flasks with 100 mL solution of metal ions of desired concentration. The entirety was agitated during a certain time at 300 rpm. Once the operation time had elapsed, the liquid phase was taken out, and then filtered through filter paper (Double Boxing rings 102) and final concentration of metal ion was determined in the filtrate by Atomic Absorption Spectrometry (AAS). The amount of metal ions adsorbed at equilibrium per unit mass of biosorbent was determined according to the following equation:

$$q_e = \frac{(C_0 - C_e) \cdot V}{m} \quad (1)$$

Where  $m$  is the mass of adsorbent (g);  $V$  is the volume of the solution (L);  $C_0$  is the initial concentration of metal (mg/L);  $C_e$  is the equilibrium concentration of the adsorbate (mg/L) in solution and  $q_e$  is the metal quantity adsorbed at equilibrium (mg/g). For the calculation of iron rate adsorption ( $R$ ), the following expression was used:

$$R(\%) = \frac{(C_0 - C_e) 100}{C_0} \quad (2)$$

### 3. Results and discussions :

#### 3.1. Characterization of adsorbent:

##### 3.1.1. FT-IR Studies:

FTIR spectra of *Luffa cylindrica* (LC) and iron sorbed LC are presented in Figure 1. A band at about  $3418 \text{ cm}^{-1}$  could be assigned to  $\text{OH}^-$  stretching vibrations. The peak at about  $2916 \text{ cm}^{-1}$  was attributed to the asymmetric and symmetric stretching vibrations of  $\text{CH}_2$  and  $\text{CH}_3$ . The band around  $1638 \text{ cm}^{-1}$  was associated with  $\text{C}=\text{C}$  and  $\text{C}=\text{O}$  stretching in the aromatic ring [9]. The peak at  $1056 \text{ cm}^{-1}$  may be due to  $\text{C}-\text{O}$  stretching vibrations [8]. Also it is important to notice that the band intensities decreased in the FTIR spectrum of iron loaded LC because the functional groups of the LC surface have been occupied with iron. This study demonstrated that iron was adsorbed and penetrated into the interlayer space of the LC.

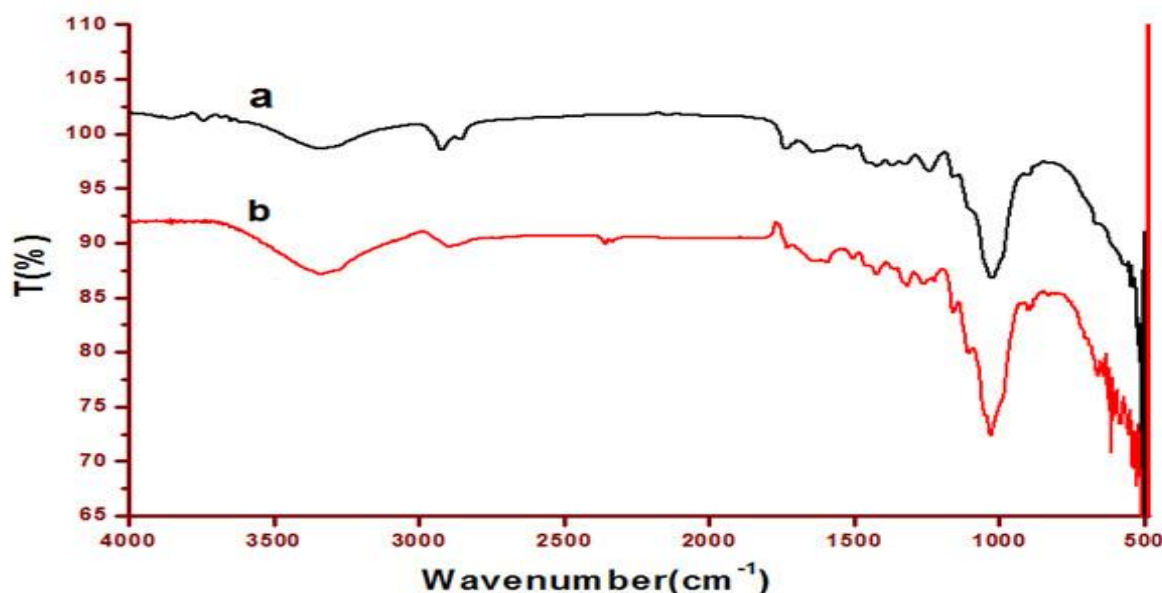


**Figure 1:** FTIR spectra of (a) raw LC fiber and (b) LC loaded iron sample

##### 3.1.2. X-Ray diffraction:

XRD patterns of LC before and after  $\text{Fe(II)}$  adsorption ( $T: 25^\circ\text{C}$ ,  $\text{pH}: 6$ ,  $C_0: 200 \text{ mg L}^{-1}$ ) are shown in Figure 2.

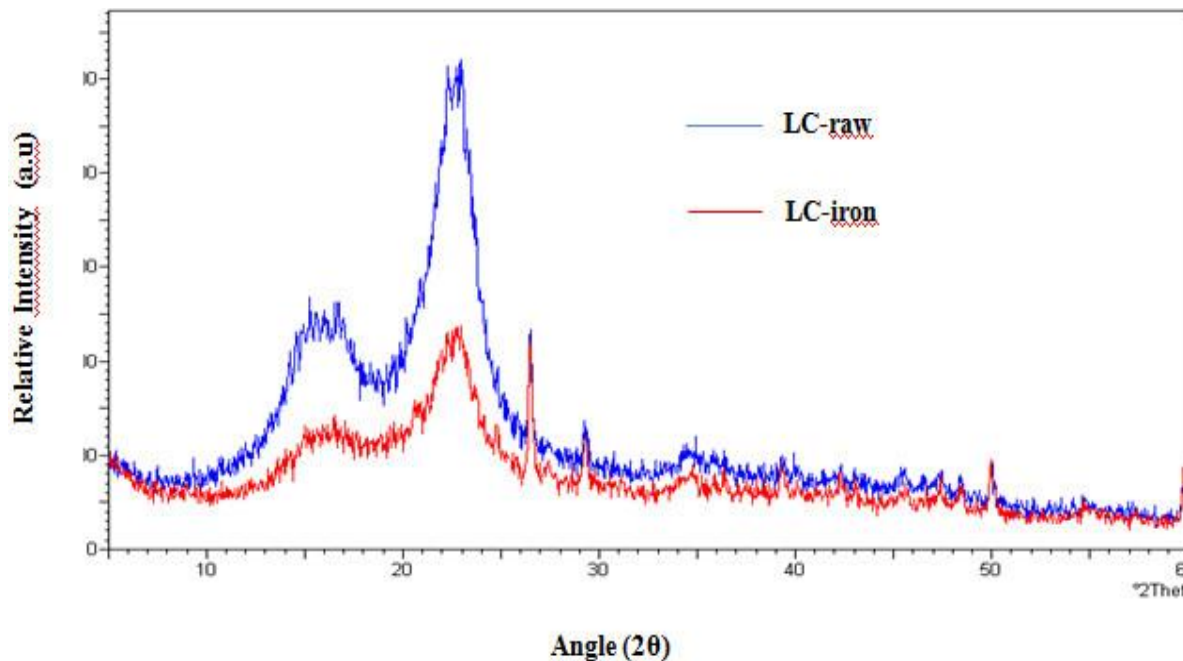


**Figure 2:** X-ray diffraction patterns of LC before (a) and after (b) adsorption.

The XRD patterns of LC raw and LC loaded with Fe (II) were shown in Figure 2. The LC raw at 2θ scale is shown peaks at 23.04° and 16.64° with relative intensities of 1145 and 519, respectively. Similarly, LC loaded with Fe (II) is shown peaks at 26.46° and 14.93° with relative intensities of 443 and 244, respectively. The percentage crystallinity (X<sub>c</sub>%) and crystallinity index (C.I.) were calculated as follows [12, 13].

$$X_c\% = \frac{I_c}{I_A + I_c} \times 100\% \quad (3)$$

$$C.I. = \frac{I_c - I_A}{I_c} \quad (4)$$

Where I<sub>c</sub> is peak intensity of crystalline phase, I<sub>A</sub> is peak intensity of amorphous phase. The percentage crystallinity of LC raw and LC fibers loaded with Fe (II) were observed as 68.8 and 64.17, while the crystallinity index as 0.56 and 0.44. It was observed that the intensity of the peak in LC loaded with Fe (II) is decreased on the adsorption. The decrease in intensity of peak during the adsorption process is indicated a decreased in crystallinity of LC loaded with Fe (II). However, the LC loaded with Fe (II) is shown broadening of the peak after adsorption due to convergence of the fibers towards more disordered system [14].

It has been observed that (Table 1) a slight decrease in percentage crystallinity of the fibers on adsorption copolymerization resulted in increase in randomness or disorder in the crystal lattice of cellulose fiber. This was due to incorporation of Fe (II) ion on the active sites of backbone during grafting and fibers became more amorphous and resulted in impaired crystalline structure [15, 16].

**Table 1:** Percentage crystallinity and crystallization index of LC raw and LC loaded with Fe (II).

Sample	2θ (°)		Intensity		X <sub>c</sub> %	C.I
	Crystalline peak	Amorphous peak	I <sub>c</sub>	I <sub>A</sub>		
LC raw	23.04	16.64	1145	519	68.81	0.54
LC loaded with Fe(II).	26.46	14.93	443	244	64.48	0.45

**3.2. Optimization of adsorption parameters:**

The optimization of different adsorption parameters such as pH of solution, Fe (II) concentration, dose of LC and particles size of LC at different time intervals was carried out for Fe (II) onto *Luffa Cylindrica*.

**3.2.1. Effect of pH:**

The pH is an important process parameter on adsorption of metal ions from aqueous solutions since it is responsible for protonation of metal binding sites. As a result the rate of adsorption will vary with pH of an aqueous medium [17]. The influence of pH solution on iron adsorption onto LC is carried out at pH range of 1-8 and shown in Figure 3. The Fe (II) removal is increased with pH 6, and then it is sharply decreased. The maximum adsorption of Fe (II) is attained at pH of 6. At pH range of 1-5, there are many positive charges on the surface of LC, these charges which are attributed to the presence of H<sup>+</sup> are competed with Fe (II) cations and hampered their adsorption, giving a large static repulsion force. As the pH is increased, the active sites which are increased the negative charge density on the LC surface would be exposed. These negative charge are increased the attraction of metallic ions with positive charge and allowed the adsorption onto the LC surface. In this study, these iron cations at around pH 6 would be expected to interact more strongly with the negatively charged binding sites in the biosorbent. As a result, the optimum pH for iron adsorption was found at pH of 6 and the other adsorption experiments were performed at this pH value.

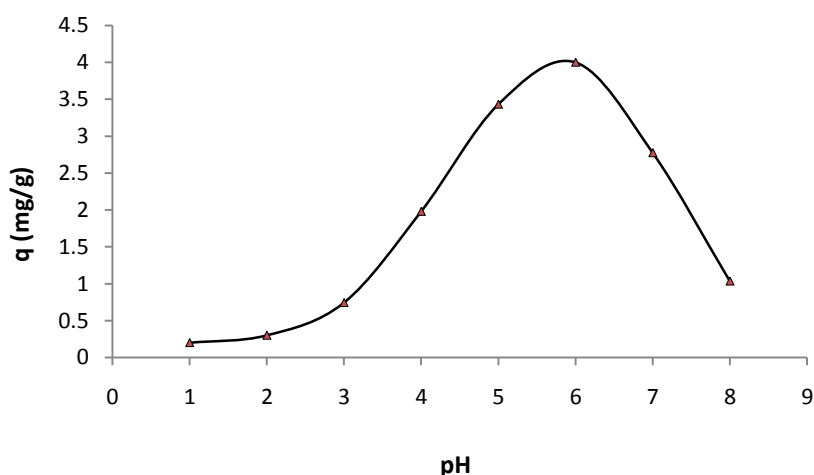


**Figure 3:** Effect of pH on iron adsorption onto LC at ( $C_0 = 100$  mg/L,  $m = 1$  g,  $T = 25$  °C, contact time = 90 min and agitation rate = 300 rpm).

**3.2.2. Effect of contact time:**

Adsorption of Fe (II) was measured at different contact times given in Figure 4 for three different initial Fe (II) concentrations of 10, 50 and 100 (mg/L).

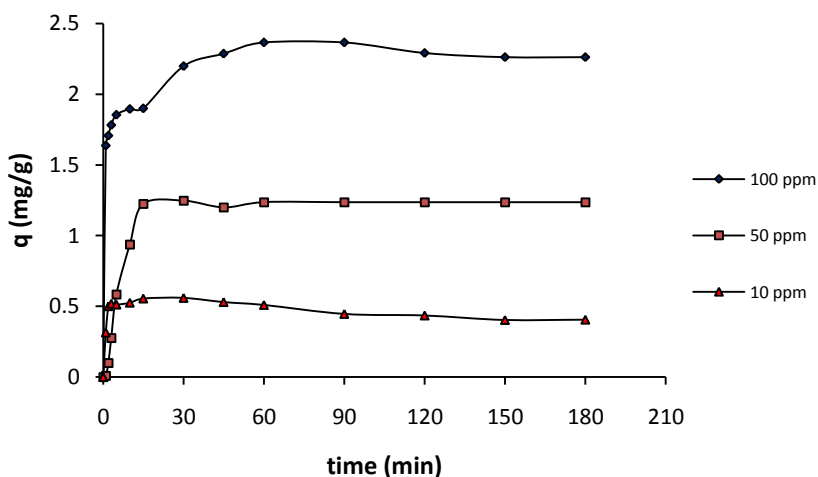


**Figure 4:** Effect of contact time iron ions adsorption onto LC at ( $C_0 = 100$  mg/L, pH=6,  $m = 1$  g,  $T = 25$ °C, contact time = 3 h and agitation rate = 300 rpm).

The curves are revealed that iron removal is higher at the beginning; which is probably due to the large surface area of the LC being available at beginning for the adsorption of Fe (II) ions. As the surface adsorption sites are become exhausted, the adsorption rate is controlled by the adsorbed amount of this metal at which the adsorbate is transported from the exterior to the interior sites of the adsorbent particles. Most of the maximum quantity iron removal is attained within 60 min (Figure 4) of agitation time at different initial concentrations. By increasing contact time, the Fe (II) adsorption is increased and remained constant after equilibrium reached in 90 min for different initial concentrations.

### 3.2.3. Effect of adsorbent dose:

The effect of the adsorbent dose on the amount adsorbed of iron was studied at 25 °C and pH of 6 by varying the adsorbent amounts from 0.2 to 7 g/L. For all these runs, initial concentration of Fe (II) ions was fixed as 100 mg/L. The analysis was shown that the adsorption of Fe (II) is increased as the adsorbent dosage increased from 0.1 to 7 g/L due to the limited availability of the adsorbing species number for a relatively larger number of surface sites on the adsorbent at higher dosage of adsorbent. It is apparent that with higher dosage of adsorbent there would be greater availability of exchangeable sites from metals ions. The significant increase in uptake was observed when the dose was increased from 0.1 to 1.5 g/L; any further addition of the adsorbent than this dose would not cause any significant change in the adsorption. These results are clearly indicated that the LC dosages must be fixed at 1.5 g/L, (Figure 5) which is the dosage that corresponding to the minimum amount of adsorbent that is led to constant Fe (II) removal. LC dosages were therefore fixed at 1.5 g/L for the entire experiments.

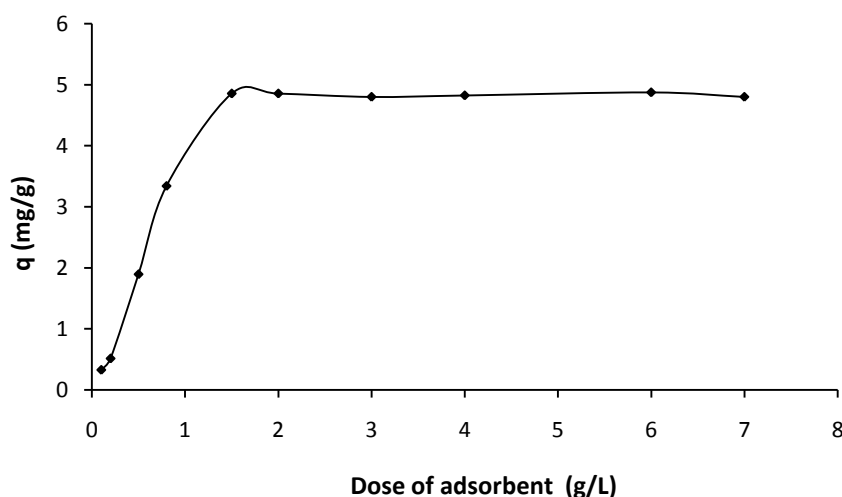


**Figure 5:** Effect of adsorbent dosage on the Fe (II) adsorption onto LC ( $C_0 = 100$  mg/L, pH=6,  $T = 25^\circ\text{C}$ , contact time = 90 min, agitation rate = 300 rpm).

### 3.2.4. Effect of particles size:

The contact surface between any biosorbent and the liquid phase is played an important role in the phenomenon of adsorption. According to Figure 6 the results are shown that the adsorbed amount of iron is increased with the reduction in the diameter of the particles, which is probably due to the increase of the number of active sites and also the increase of the biosorbent surface. The maximum removal rate of (63.42%) was reached using the fine particle (diameter less than 0.063 mm).

### 3.3. Adsorption isotherm models:

The adsorption isotherm represents the quantity adsorbed according to the concentration of the aqueous solution to equilibrium at a given temperature. Firstly the isotherms models of adsorption are generally used to describe the interactions between the adsorbate and the adsorbent when the process of adsorption reaches equilibrium. Secondly, they make it possible to extract the important parameters for the systems design from adsorption. The data of adsorption were analyzed by the two models of Freundlich and Langmuir [6]. Adsorption of Fe (II) ions onto LC particles was modeled using four adsorption isotherms.

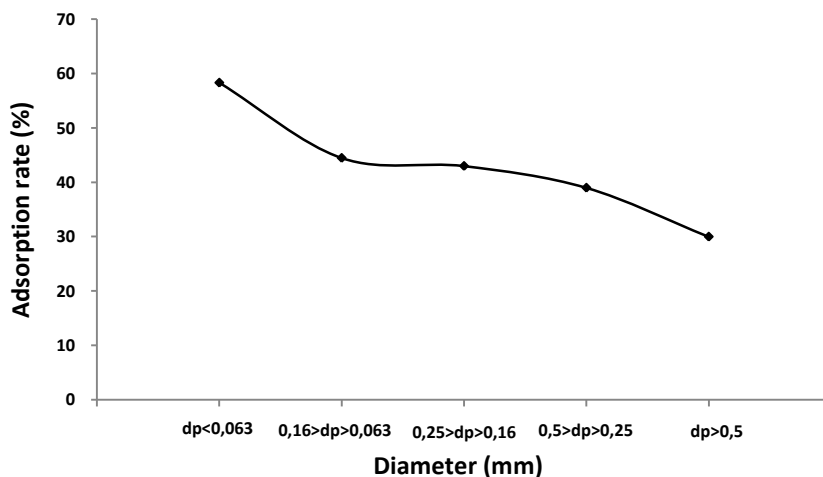


**Figure 6:** Effect of the diameter of biosorbent particle (dp) on iron adsorption onto LC at ( $C_0 = 100$  mg/L, pH=6, m=1g; T = 25°C, contact time = 90 min and agitation rate = 300 rpm).

1

### 3.3.1. Freundlich isotherm:

The Freundlich isotherm model is the well known earliest relationship describing the adsorption process. This model applies to adsorption on heterogeneous surfaces with the interaction between adsorbed molecules and the application of the Freundlich equation also suggests that adsorption energy exponentially decreases on completion of the biosorptional centers of an adsorbent. This isotherm is an empirical equation and can be employed to describe heterogeneous systems and is expressed as follows in linear form [18]:

$$\log q_e = \log K_F + \frac{1}{n} \log C_e \quad (5)$$

Where  $K_F$  is the Freundlich constant related to the bond Phoning energy.  $1/n$  is the heterogeneity factor and  $n$  (g/L) is a measure of the deviation from linearity of adsorption. Freundlich equilibrium constants were determined from the plot of  $\log q_e$  versus  $\log C_e$ , Figure 7 on the basis of the linear of Freundlich equation (5). The  $n$  value indicates the degree of non-linearity between solution concentration and adsorption as follows: if  $n = 1$ , then adsorption is linear; if  $n < 1$ , then adsorption is a chemical process; if  $n > 1$ , then adsorption is a physical process. The  $n$  value in Freundlich equation was found to be 1.26–1.42 for LC, Table 3. Since  $n$  lie between 1 and 10, this indicates the physical adsorption of iron (II) onto LC. The values of regression coefficients  $R^2$  are regarded as a measure of goodness of fit of the experimental data to the isotherm models.

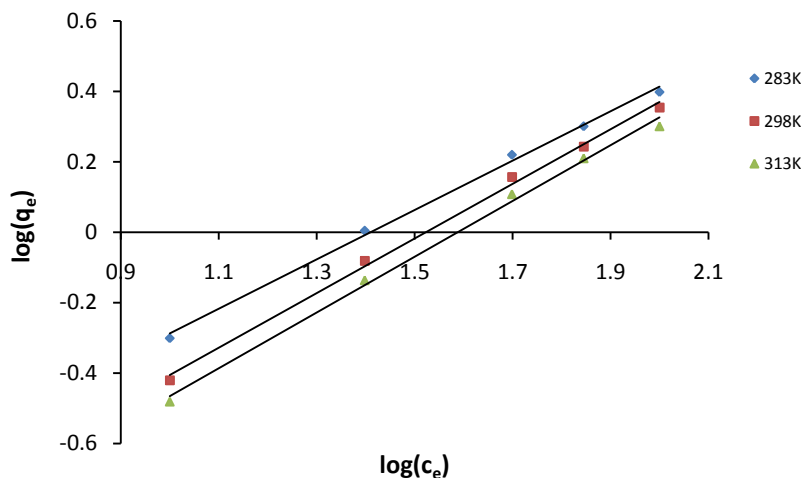


**Figure 7:** Freundlich isotherm for Fe (II) adsorption onto LC.

### 3.3.2 Langmuir isotherm:

The Langmuir isotherm assumes monolayer adsorption on a uniform surface with a finite number of adsorption sites [19]. Once a site is filled, no further adsorption can take place at that site. As such the surface will eventually reach a saturation point where the maximum adsorption of the surface will be achieved. The linear form of the Langmuir isotherm model is described as:

$$\frac{C_e}{q_e} = \frac{1}{K_L \cdot q_{\max}} + \frac{1}{q_{\max}} C_e \quad (6)$$

Where  $K_L$  is the Langmuir constant related to the energy of adsorption and  $q_{\max}$  is the maximum adsorption capacity (mg/g). Values of Langmuir parameters  $q_{\max}$  and  $K_L$  were calculated from the slope and intercept of the linear plot of  $C_e/q_e$  versus  $C_e$  as shown in Figure 8. Values of  $q_{\max}$ ,  $K_L$  and regression coefficient  $R^2$  are listed in Table 2. These values for LC biosorbent indicated that Langmuir theory describes the adsorption phenomena favorable.

The essential characteristics of the Langmuir isotherm parameters can be used to predict the affinity between the adsorbate and adsorbent using separation factor or dimensionless equilibrium parameter, “ $R_L$ ”, expressed as in the following equation [20]:

$$R_L = \frac{1}{(1 + K_L C_o)} \quad (7)$$

Where  $K_L$  is the Langmuir constant and  $C_o$  is the initial concentration of Fe (II) ions. The value of separation parameter  $R_L$  provides important information about the nature of adsorption. The value of  $R_L$  indicated the type of Langmuir isotherm to be irreversible ( $R_L = 0$ ), favorable ( $0 < R_L < 1$ ), linear ( $R_L = 1$ ) or unfavorable ( $R_L > 1$ ). The  $R_L$  was found to be 0.5–0.57 for concentration of 10– 100 mg/L of Fe (II). They are in the range of 0–1 which indicates the favorable adsorption.

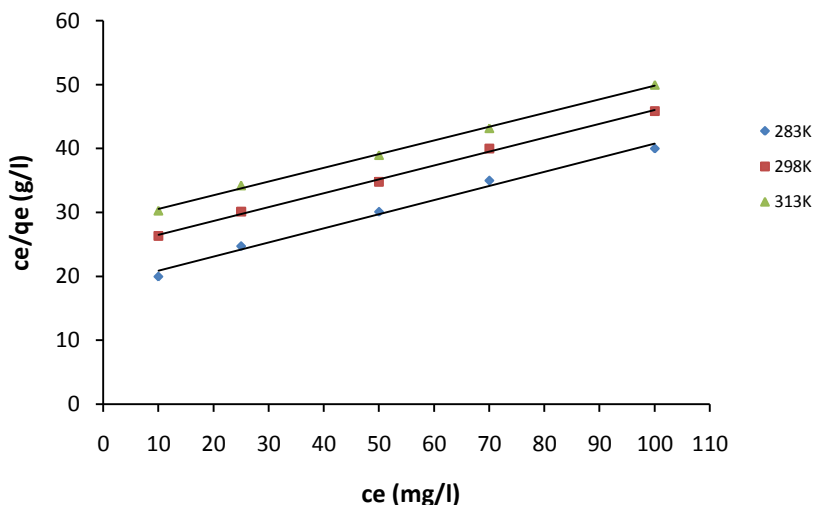


**Figure 8:** Langmuir isotherm for Fe (II) adsorption onto LC.

### 3.3.3 Temkin isotherm:

The Temkin isotherm model assumes the adsorption energy decreases linearly with the surface coverage due to adsorbent–adsorbate interactions. The linear form of Temkin isotherm model [21, 22] is defined by:

$$q_e = RT \ln K_T + \frac{RT}{b_T} \ln C_e \quad (8)$$

Where  $b_T$  is the Temkin constant related to heat of adsorption (J/mol) and  $K_T$  is the Temkin isotherm constant (L/g). These constants were obtained from plotting  $q_e$  versus  $\ln(C_e)$ , Figure 9. Values of  $b_T$  and  $K_T$  are listed in Table 2.

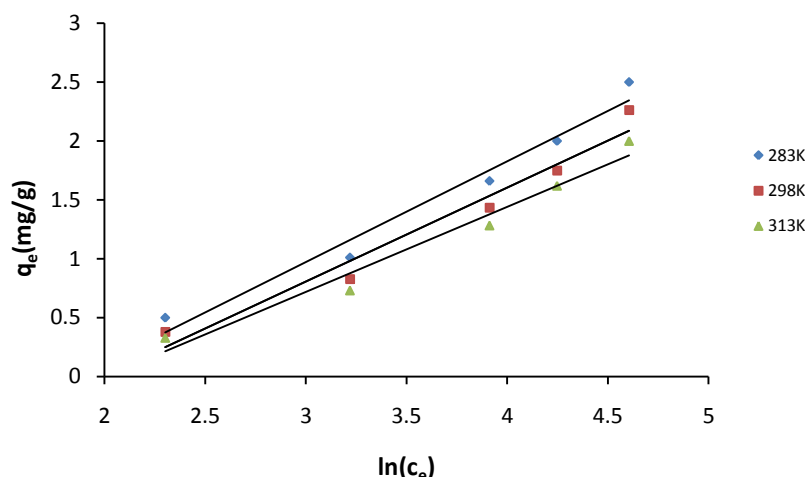


**Figure 9:** Temkin isotherm for Fe (II) adsorption onto LC.

**3.3.4 Dubinin–Radushkevich (D–R) isotherm:**

The D–R isotherm model is a semi-empirical equation where adsorption follows a pore filling mechanism. It assumes that the adsorption has a multilayer character, involves Van der Waals forces and is applicable for physical adsorption processes. The linear form of D–R isotherm model [23] is expressed as:

$$\ln q_e = \ln q_d - \beta \epsilon^2 \tag{9}$$

Where  $q_d$  is the D–R constant (mg/g),  $b$  is the constant related to free energy and  $e$  is the Polanyi potential which is defined as:

$$\epsilon = RT \ln \left( 1 + \frac{1}{c_e} \right) \tag{10}$$

The Polanyi potential  $\epsilon$  was determined from Equation (10). The calculated  $q_d$  and  $\beta$  constants in Equation (9), Table 2 were determined from intercept and slope of a plot of  $\ln q_e$  versus  $\epsilon^2$ .

From the data in Table 2, it was observed that Langmuir model showed a better fit than the Freundlich isotherm, Temkin equation, and Dubinin–Radushkevich (D–R) equation, thus indicating the applicability of monolayer coverage of iron (II) ions on (LC) surface. Also the equilibrium data were also well described by Temkin equation, (Table 2).

**Table 2:** Langmuir, Freundlich, Temkin and Dubinin–Radushkevich constants for Fe (II) adsorption onto LC.

T (K)	Langmuir			Freundlich			Temkin			D–R		
	$q_{max}$ (mg/g)	K (L/mg)	$R^2$	$K_L$ (mg/g)	1/n	$R^2$	$b_T$ (j/mole)	$K_T$ (L/g)	$R^2$	$q_d$ (mg/g)	B	$R^2$
283	4.52	0.01	0.989	0.102	0.701	0.997	2754.1	0.9993	0.971	1.88	-3E-05	0.844
298	4.60	0.0089	0.990	0.065	0.775	0.976	3105.5	0.9993	0.962	1.64	-3E-05	0.845
313	4.65	0.0075	0.998	0.055	0.792	0.966	3603.7	0.9994	0.967	1.47	-3E-05	0.847

**3.4. Kinetic studies:**

A quantitative understanding of the adsorption is possible with the help of kinetic models. The pseudo-first-order kinetic model, as expressed by [24], can be written as:

$$\log(q_e - q_t) = \log q_e - K_1 \cdot t / 2.303 \tag{11}$$

Where  $q_e$  and  $q_t$  are the amounts of metal adsorbed ( $\text{mg.g}^{-1}$ ) at equilibrium and at time  $t$ , respectively, and  $k_1$  is the pseudo-first-order equilibrium rate constant ( $1/\text{min}$ ). A plot of  $\log(q_e - q_t)$  versus  $t$  gives straight line confirming the applicability of the pseudo-first-order rate equation.

Pseudo-second-order adsorption rate equation [25] may be expressed as follows:

$$\frac{t}{q_t} = \frac{1}{k_2 q_e^2} + \frac{1}{q_e} t \quad (12)$$

$k_2$  is the Pseudo-second-order adsorption rate constant ( $\text{g/mg.min}$ ). Straight line plot of  $t/q_t$  v  $t$  indicates the applicability of Pseudo-second-order model.

**Table 3** Kinetic and diffusion parameters for adsorption of iron onto LC at different initial iron concentrations.

The

Iron conc. (mg/L)	Experimental	Pseudo-first-order			Pseudo-second-order		
	$q_{e,\text{exp}}$ (mg/g)	$q_{e,\text{cal}}$ (mg/g)	$k_1$ (1/min)	$R^2$	$q_{e,\text{cal}}$ (mg/g)	$k_2$ (g/mg.min)	$R^2$
25	0.68	0.50	0.0366	0.96	0.70	0.21	0.99
50	0.93	0.80	0.029	0.96	0.98	0.13	0.98
100	3.17	0.90	0.025	0.98	3.17	0.1	0.99

experimental results of the Fe (II) uptake,  $q_t$  versus  $t$  were fitted to the models mentioned above by the method of nonlinear regression. The results are shown in Table 3 and Figure 10 and 11. Theoretical values ( $q_{e,\text{cal}}$ ) were almost equivalent to those of the experimental data ( $q_{e,\text{exp}}$ ) and low correlation coefficient values obtained for the Pseudo-first-order model were indicated that adsorption is not occurred exclusively on one site per ion. The comparison of experimental adsorption capacities and the theoretical values estimated from the first- and second-order equation are presented in Table 3. All the  $R^2$  values are close to “one”, confining the applicability of the Pseudo-second-order equation. The values of the rate constants are varied with the initial concentration. Although consistency is expected for these values when a single controlling mechanism is assumed by the model, variations do occur for natural biosorbents and are usually attributed to the heterogeneous nature of the biosorbent surface. Moreover, it was noted from the regression data in Table 3 that the values of  $q_{e,\text{cal}}$ , obtained from the Pseudo second order model, are almost equivalent to the experimental results of  $q_{e,\text{exp}}$ , obtained from Lagergren’s model. Furthermore, for different concentrations of Fe (II), the constants calculated from the plots are given in Table 3. The  $R^2$  values are excellent and theoretical values of  $q_{e,\text{cal}}$  match well with those of experimental data. Therefore, the adsorption of Fe (II) onto LC is followed the Pseudo-second-order reaction kinetics.

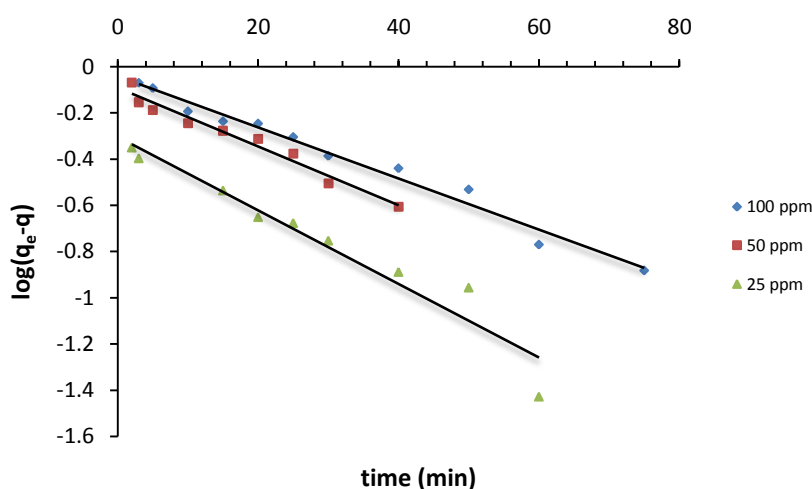


**Figure 10:** Pseudo-first order kinetic model for Fe (II) adsorption onto LC at different initial concentrations.

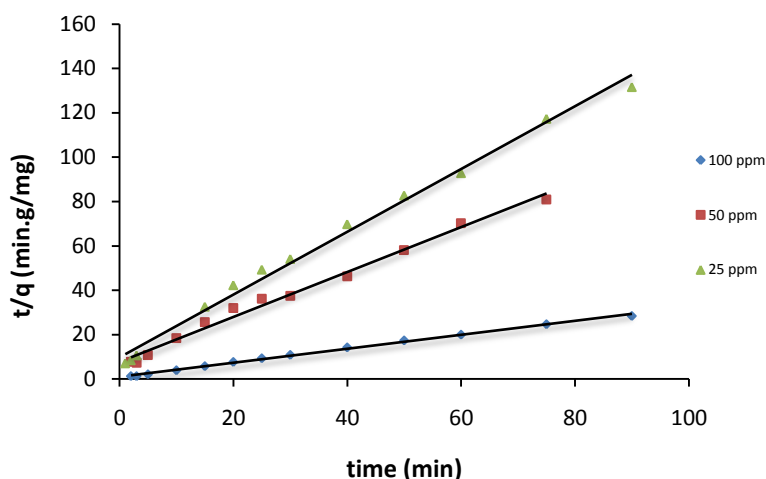


**Figure 11:** Pseudo-second order kinetic model for Fe (II) adsorption onto LC at different initial concentrations

### 3.6. Thermodynamic study:

Thermodynamic parameters such as standard free energy change ( $\Delta G^\circ$ ), standard enthalpy change ( $\Delta H^\circ$ ) and standard entropy change ( $\Delta S^\circ$ ) can be calculated using the following equation [26]:

$$\ln K_c = -\frac{\Delta G^\circ}{RT} = \frac{\Delta S^\circ}{R} = -\frac{\Delta H^\circ}{RT} \quad (14)$$

Where,  $K_c$  is equilibrium constant resulting from the ratio of the equilibrium concentrations of the Fe (II) on an adsorbent in the solution. ( $\Delta G^\circ$ ), ( $\Delta H^\circ$ ) and ( $\Delta S^\circ$ ) can be calculated from a plot of  $\ln(K_c)$  versus  $1/T$ .

The thermodynamic parameters of the Fe (II) adsorption onto LC are given in Table 4. The standard Gibbs free energies ( $\Delta G^\circ$ ) of adsorption were negative at all investigated temperatures. The negative values of  $\Delta G^\circ$  of the adsorption are confirmed that the adsorption of Fe (II) onto LC was feasible and spontaneous [27]. In addition, the ( $\Delta G^\circ$ ) values increased when the temperature increased, suggesting that adsorption might be more spontaneous at lower temperature. Generally, the range of free energy values ( $\Delta G^\circ$ ) for physisorption is between 20 and 0 kJ/mol, while chemisorption is between 80 and 400 kJ/mol [28]. This further is indicated that the adsorption of the Fe (II) onto LC was by physisorption. The change in adsorption standard enthalpy ( $\Delta H^\circ$ ) for Fe (II) adsorbed onto LC was -9.502 kJ/mol, indicating loose bonding between the Fe (II) and LC since Fe (II) was adsorbed and penetrated into the interlayer space of adsorbent, indicating that the adsorption process was exothermic [28]. The adsorption of Fe (II) onto LC can be concluded to be via physisorption. Since the change in the standard enthalpy is less than 40. KJ/mol [29]. The standard entropy change ( $\Delta S^\circ$ ) for Fe (II) adsorbed onto LC was -0.027 KJ/mol. The negative value of ( $\Delta S^\circ$ ) suggested a decrease in degree of freedom of the adsorbed Fe (II) [27].

**Table 4:** Thermodynamic parameters of adsorption of Fe (II) onto LC.

Temperature (K)	$\Delta G^\circ$ (KJ/mol)	$\Delta S^\circ$ (KJ/mol)	$\Delta H^\circ$ (KJ/mol)
283	-1.866		
298	-1.461	-0.027	-9.502
313	-1.056		

### Conclusions

The present study showed that the LC is a cheap biosorbent available abundantly in Algeria. The adsorption of iron onto Luffa Cylndrica fibers cords was studied. It has been established that this biosorbant has an acceptable adsorption capacity towards the toxic metal ions. The adsorption of Fe (II) was found to be dependent on the time of contact, pH, initial concentration, effect of masse and particles size. The removal rate

was increased with increasing contact time and the equilibrium was reached in 90 min. The maximum removal of Fe (II) was attained at pH of 6, at this pH, the removal rate of iron ions was found to be 52.2%, LC dose of 1.5 g/L using Fe (II) concentration of 100mg/L. The extent of the removal of iron is highly dependent on the particles size of LC. It was observed that the removal rate increases with the decrease of the diameter of the biosorbent in the suspension. The equilibrium adsorption data were best represented by the Langmuir isotherm, indicating monolayer adsorption on a homogenous surface and the values of  $q_{max}$  were increased from 2.51 to 4.97 mg/g at 25 °C. The adsorption kinetic was well described by the Pseudo-second-order model. The adsorption is more spontaneous at lower temperatures, tends to be exothermic. The FT-IR analysis indicates that after adsorption the pores of the adsorbent were saturated with iron. X-ray diffraction results indicate the low values of percentage crystallinity and crystallinity index for LC loaded with Fe (II).

## References

1. Momteiro L. P. C.; Mainier F. B., *Engevista*. 12 (2010) 33.
2. Prapti U. Shah., Nirav P. Raval., Nisha K. Shah. *J. Mater. Environ. Sci.*, 6 (2015) 2573.
3. San Francisco, Arms K Environmental Science, CA: *Saunders College, New York*, 1990.
4. R. Lauffer, Iron and Human diseases, *CRC Press, London.*, 1992.
5. T. Emery, Iron and your health: Facts and fallacies, *CRC Press, London.*, 1991.
6. Ksakas A., Loqman A., El Bali B., Taleb M., Kherbeche A., *J. Mater. Environ.*, 6 (2015) 2003.
7. Abdelwahab O., Amin N.K., *Egyptian Journal of Aquatic Research.*, 39 (2013) 215.
8. Gupta V.K., Agarwal S., Singh P., Pathania D., *Carbohydr. Poly.*, 98 (2013) 121.
9. Tanobe V.O.A., Sydenstricker T.H.D., Munaro M., Amico S.C., *Polym.*, 24 (2005) 474.
10. Demir H., Top A., Balkose D., Ulku S., *J. Hazard. Mater.*, 153 (2008) 389.
11. Ad C., Benalia M., Laidani Y., Elmsellem H., Ben Saffedine F., Nouacer I., Djedid M., El Mahi B., Hammouti B., *Der Pharma Chemica.*, 12 (2015) 388.
12. Kalia S., Kumar A., & Kaith B.S., *Advanced Material Letters*, 2 (2010) 17.
13. Sanghavi B.J., Mobina S.M., Mathur P., Lahiri G. K., & Srivastava A. K., *Biosensors and Bioelectronics.*, 39 (2013) 124.
14. Sanghavi B. J., Kalambate P. K., Karna S. P., & Srivastava A. K., *Talanta.*, 120 (2014) 1.
15. Sharma S., Pathania D., *Advanced Materials Letters*, 4 (2013) 271.
16. Wang L., Dong W., & Xu Y., *Carbohydrate Polymers*, 68 (2006) 626.
17. Senturk H., Ozdesa D., Gundogdu A., Duran C., Soy lak M., *J. Hazard. Mater.*, 172 (2009) 353.
18. Freundlich H., Am J., *Chem. Soc.*, 61 (1939) 2.
19. Langmuir I., Amer J., *Chem. Soc.*, 40 (1918) 1361.
20. Ozer A., Ozer D., Ozer A., *Process Biochem.*, 39 (2004) 2183.
21. Aharoni A., Ungarish M., *J. Chem. Soc. Faraday Trans.*, 73 (1977) 456.
22. Boparai H.K., Joseph M., O'Carroll D.M., *J. Hazard. Mater.*, 186 (2011) 458.
23. Huston N.D., Yang R.T., *Adsorption*, 3 (1997) 189.
24. Lagergren S., Sven K., *Vetenskapsakad. Handl.*, 24 (1898) 1.
25. Ho Y.S., Wase D.A., Forster C.F., *Environ. Technol.*, 17 (1996) 71.
26. Liu Z., Zeng Z., Zeng G., Li J., Zhong H., Yuan X., Liu Y., Zhang J., Chen M., Liu Y., Xie G., *Technol.*, 110 (2012) 468.
27. Fu Q.L., Deng Y.L., Li H.S., Liu J., Hua H.Q., Chen S.W., Sa T.M., *Appl. Surf.*, 255 (2009) 4551.
28. Su J., Lin., Hong-fu., Wang, Qing-Ping., Xie, Zheng-Miao., Chen, Zuliang., *Desalination*, 269 (2011) 163.
29. Canizares P., Carmona M., Baraza O., Delgado A., Rodrigo M.A., *J. Hazard. Mater.*, 131 (2006) 243.

(2016) ; <http://www.jmaterenvirosci.com>